Published in final edited form as:
Mol Cancer Res. 2012 June ; 10(6): 810–820. doi:10.1158/1541-7786.MCR-11-0576.

PRAK suppresses oncogenic *ras*-induced hematopoietic cancer development by antagonizing the JNK pathway

Naoto Yoshizuka[1], **Maoyi Lai**[2], **Rong Liao**[1], **Ryan Cook**[2], **Changchun Xiao**[2], **Jiahuai Han**[3], and **Peiqing Sun**[1,*]

[1]Department of Molecular Biology, The Scripps research Institute, La Jolla, CA 92037

[2]Department of Immunology and Microbial Science, The Scripps research Institute, La Jolla, CA 92037

[3]State Key Laboratory of Cellular Stress Biology and School of Life Sciences, Xiamen University, Xiamen, Fujian 361005, China

Abstract

The p38 MAPK pathway regulates multiple physiological and pathological processes, including cancer development. PRAK, a p38 substrate protein kinase, has previously been implicated in the suppression of skin carcinogenesis. In the current study, we demonstrate that PRAK deletion accelerates hematopoietic cancer development in a mouse model harboring an oncogenic *ras* allele, *Eμ-N-Ras*^{G12D}, specifically expressed in hematopoietic cells. Further investigation reveals that enhanced hematopoietic tumorigenesis by PRAK deficiency is associated with hyper-activation of the JNK pathway both in vivo and in primary hematopoietic cells isolated from spleens. In primary splenocytes, PRAK deficiency further enhanced oncogenic *ras*-induced cell proliferation, and promoted *ras*-mediated colony formation on semi-solid medium in a JNK-dependent manner. In addition, deletion of PRAK leads to abrogation of *ras*-induced accumulation of senescence markers. These findings indicate that PRAK suppresses hematopoietic cancer formation in this mouse model by antagonizing oncogenic *ras*-induced activation of the JNK pathway. Our results suggest that PRAK may function as a tumor suppressor in multiple types of cancers.

Keywords

PRAK; ras; JNK; lymphomagenesis; oncogene-induced senescence; mouse cancer model

Introduction

The p38 MAPK was initially identified as a mediator of inflammation and stress responses (1-4). Recent studies have revealed a novel function of the p38 pathway in tumor suppressing cellular responses such as oncogene-induced senescence, cell contact inhibition and DNA damage responses (5). These findings suggest that p38 has a tumor-suppressing function. Indeed, tissue-specific deletion of p38α promotes the development of chemical-induced liver cancer and *K-ras*^{G12V}-induced lung cancer in mice (6, 7). Moreover, deletion of Wip1, a p38 phosphatase frequently amplified in human breast tumors, leads to p38 activation and reduced erbB2- and *ras*-mediated mammary tumorigenesis in mice (8, 9).

*Correspondence should be addressed to: Department of Molecular Biology, The Scripps Research Institute, 10550 N. Torrey Pines Rd, MB-41, La Jolla, CA 92037. Tel: 858-784-9710; FAX: 858-784-9067; pqsun@scripps.edu. .

Like other MAPK pathways, the functions of p38 are mediated by its downstream substrates. Numerous p38 substrates, including serine/threonine protein kinases, transcription factors and cell-cycle regulators, have been identified that mediate various p38 functions (10). The p38 downstream kinase substrates include MAPK-activated kinases 2 (MK2) and 3 (MK3), MAPK-interacting protein kinase 1 (MNK1), p38-regulated/activated kinase (PRAK), mitogen- and stress-activated protein kinases-1 (MSK1) and -2 (MSK2), and casein kinase 2 (CK2). Upon phosphorylation by p38, these Ser/Thr protein kinases activate substrates such as heat shock proteins, transcription factors, translation initiation factors, and proteins that regulate mRNA stability. In a previous study, we demonstrated that the ability of p38 to mediate oncogene-induced senescence and tumor suppression relies, at least in part, on its downstream substrate kinase PRAK, also known as MAPK-activated protein kinase 5 (MK5). Replicative senescence is a stable proliferative arrest associated with the exhaustion of replicative potential as a result of telomere erosion during cell divisions (11). Telomere length-independent, senescence-like proliferative arrest can also be induced in young cells by activated oncogenes such as *ras* (12). This second type of arrest state is thus operatively termed as oncogene-induced premature senescence. Like apoptosis, oncogene-induced senescence serves as an anti-tumorigenic defense mechanism (13-16). Our studies revealed that PRAK is essential for *ras*-induced senescence, and that PRAK deficiency disrupts oncogene-induced senescence and enhances DMBA-induced skin carcinogenesis (17).

While our previous results indicate that PRAK suppresses skin carcinogenesis (17), it is unclear whether the tumor suppressing activity of PRAK also operates in other types of cancers. To this end, the consequence of PRAK inactivation was analyzed in the current study using an *N-ras*^{G12D} transgenic mouse model previously shown to develop hematopoietic cancer (15). Our data demonstrate that PRAK deletion also accelerates tumor formation in this *N-ras*^{G12D} transgenic line, and enhances cell proliferation and soft agar colony formation induced by activated *ras* in primary splenocytes. Further studies indicate that enhanced hematopietic tumorigenesis by PRAK deficiency is accompanied by hyper-induction of the JNK pathway and downregulation of a subset of senescence markers, and that inhibition of JNK activity attenuates the hyper-proliferation induced by oncogenic *ras* in hematopoietic cells isolated from PRAK deficient mice. These findings suggest that PRAK may suppress the development of a broad range of cancers, and that in the case of *ras*-induced hematopoietic cancer, the tumor-suppressing function of PRAK may be attributed to its ability to antagonize the activation of tumor-promoting MAKP pathways by oncogenic *ras*.

Materials and Methods

Mouse strains

The *Eμ-N-Ras*^{G12D} transgenic strain (18) was inter-crossed with mice harboring a targeted deletion in the *PRAK* gene (17) to generate the *Eμ-N-Ras*^{G12D}*;PRAK*$^{+/-}$ line (F1), which was then crossed with *PRAK*$^{+/-}$ to obtain *Eμ-N-Ras*^{G12D}*;PRAK*$^{+/+}$, *Eμ-N-Ras*^{G12D}*;PRAK*$^{+/-}$, and *Eμ-N-Ras*^{G12D}*;PRAK*$^{-/-}$ littermates (F2) for observation of hematopietic cancer development. The mice were in the BL6/129 background. All the mice carried only one copy of the *ras* transgene, as the F1 mice were heterozygous for the transgene. Animals were genotyped by allele-specific PCR as described previously. Time to death was defined as the latency between birth and death or a terminal disease stage as indicated by symptoms of severe sickness (lethargy, distress, swollen neck, abdominal bulging, and etc.). Statistical analysis of Kaplan-Meier survival plots is based on the log-rank (Mantel-Cox) test. After euthanasia of mice with deep anesthesia by CO_2, tissues were processed for histopathology and subsequent staining with hematoxylin and eosin. Cardiac

or tail vein blood was collected into Microvette tubes (Sarstedt) and analyzed by a Hemavet 950 (Drew Scientific).

Immunogenotyping of hematopoietic tumor cells

Organs such as spleen, thymus, and bone marrow were isolated from mice and minced in PBS. The mixture was then filtered through a 70-μm nylon mesh (BD Falcon) to obtain single-cell suspensions. Isolated cells were stained with antibodies against CD11b (R-Phycoerythrin conjugated) and GR-1 (Tri-color conjugated), or CD3 (R-Phycoerythrin conjugated) and B220 (Tri-color conjugated) (Caltag Laboratories), and analyzed by flow cytometry.

Isolation of primary splenocytes and transduction with recombinant retroviruses ex vivo

Spleen from 8-12-week-old non-transgenic mice served as the source for primary splenocyte preparations. Isolated spleens were minced in PBS, filtered through a 70-μm nylon mesh to obtain single-cell suspensions. Erythrocytes were removed by incubating the cell suspension with Ack buffer (0.15 M NH_4Cl, 1 mM $KHCO_3$ and 0.1 mM EDTA). The primary splenocytes were cultivated in a medium containing 45 % Iscove's MEM, 45 % Dulbecco's MEM, 10 % fetal bovine serum, 4 mM L-Glutamine, 100 U/ml Pen-strep and 25 μM β-mercaptoethanol (cell culture grade, Life Technologies). The medium was conditioned for 2-3 days on IR-irradiated (20 Gy) NIH3T3 cells before added to splenocytes.

Two retroviruses encoding shRNA targeting both JNK1 and JNK2 (shJNK1/2-S1 and – S2) were based on a published paper (19), and have the following targeting sequences, 5′-AAA GAA UGU CCU ACC UUC UTT-3′ and 5′-AGA AGG UAG GAC AUU CUU UTT-3′, respectively. Retroviruses encoding JNK1/2 shRNA, H-Ras^{G12V} (MSCV-puro-H-Ras^{G12V}) or N-Ras^{G12D} (MSCV-puro-N-Ras^{G12D}) or corresponding vector controls were packaged in an ecotropic packaging cell line LinX-E as described previously (20, 21), except that the viruses were produced in the NIH3T3-conditioned splenocyte medium. 1×10^6 freshly isolated splenocytes were mixed with 2 ml of viral supernatant in the presence of 4 μg/ml polybrene, plated onto 6-well plates and centrifuge at 2,700 rpm for 3hrs. After incubation at 32 °C for overnight, cells were subjected to a second round of retroviral infection, and then collected by centrifugation and resuspended in NIH3T3-conditioned splenocyte medium. Cells transduced with the retroviruses were selected with 1 μg/ml puromycin or 50 μg/ml hygromycin B.

Analysis of the proliferation and colony forming ability of splenocytes cultured ex vivo

To measure the rate of proliferation, primary splenocytes transduced with oncogenic *ras* or vector control were seeded onto 12-well plates in triplicates at a density of 1 to 5×10^4 cells/well in NIH3T3-conditioned splenocyte medium. Cells were harvested 4-8 days later and their numbers counted in hemocytometer. To measure colony formation on semi-solid medium, 1 to 5×10^4 of splenocytes were resuspended in the NIH3T3-conditioned splenocyte medium containing 0.3% low-melting-point agarose and plated onto a solidified bottom layer medium containing 0.5% agarose in 6-well plates, in triplicates. Colonies were photographed after 2-3 weeks, stained with 0.02% Giemsa in PBS, and counted. When necessary, 2 μM of SP600125, a JNK-specific inhibitor, or DMSO was included in the medium.

Immunohistochemical analysis

Frozen tissue samples were sliced into 8-μm sections and stored in –80 °C until use. Frozen sections were fixed in 4% buffered paraformaldehyde at 4 °C for 10 minutes, and incubated with primary antibodies (anti-Ki-67, Thermo Scientific, or anti-phospho-JNK-T183/Y185,

Cell Signaling) at 4 °C for overnight. Signals were detected by Vectastatin ABC kit (Vector Laboratories). Samples were counterstained with hematoxylin (Vector Laboratories). Positive cells were quantified under microscope in 20 randomly chosen 40X-fields.

Western blot analysis

Cells were lysed with protein lysis buffer (10 mM Tris HCl, pH 8.0, 140 mM sodium chloride, 1% Triton X-100, 1% sodium deoxycholate, and 0.1% SDS) supplemented with 1 mM sodium orthovanadate, 10 mM sodium fluoride, 1 mM β-Glycerophosphate, and Complete protease inhibitor cocktail (Roche). Cleared cell lysates were mixed with Laemmli sample buffer supplemented with β–mercaptoethanol, and boiled for 5 minutes. Equal amount of protein from the cell lysates were fractionated on SDS-PAGE, and transferred to the nitrocellulose membrane (Bio-Rad). The antibodies used in this study were purchased from BD Pharmingen (cyclin D1), Cell Signaling (phospho-JNK-T183/Y185, JNK, c-Jun, phospho-AKT-S473, AKT, phospho-ERK-T202/Y204, and ERK2), Santa Cruz (p53, Ras C-20, $p19^{ARF}$, and $p16^{Ink4a}$-M-156), Sigma (actin), and Stressgen (DcR2). The antibodies against PRAK was described previously (17). Antibody against mouse p53 phosphorylated at S37 was a gift from Dr. Carol Prives.

Quantitative real-time PCR

RNA was isolated from cells using TRIzol (LifeTechnologies). cDNA was synthesized with iScript RT Supermix (BioRad), and quantified by real-time PCR using SsoFast SYBR Green Supermix (BioRad) on a CFX96 Real-Time System (BioRad). The primers used for Grap2 were 5′-AAGGCCTCTCTCGACATCAA-3′ and 5′-AGATGGACGTTGTCCGGTAG-3′(6).

Results

PRAK deletion facilitates oncogenic *ras*-induced hematopoietic tumor development

Our previous study indicated that PRAK suppresses skin carcinogenesis induced by an environmental carcinogen DMBA(17). To evaluate the role of PRAK in hematopoietic tumor formation, we crossed the PRAK-targeted mice with the *Eμ-N-Ras*^{G12D} transgenic line harboring an activated *N-Ras*^{G12D} transgene under the control of the immunoglobulin (Ig) heavy chain (Eμ) promoter, which is expressed specifically in hematopoietic cells (18). Western blot analysis indicated that the *ras* transgene was expressed at 3-to 4-fold above the endogenous level (Figure 1A, insert). These mice develop hematopoietic tumors of myeloid and T-lymphoid origins. It was reported that targeted deletion of *p53* or *Suv39h1*, a histone methyltransferase involved in *ras*-induced senescence, promotes tumor development in these mice (15).

We monitored cancer development among $PRAK^{+/+}$, $PRAK^{+/-}$ and $PRAK^{-/-}$ littermates carrying the *Eμ-N-Ras*^{G12D} transgene. The $PRAK^{+/+}$ mice developed hematopoietic tumors in a time frame consistent with previous reports (15, 18). The median tumor-free survival of these mice was 236 days. Tumor development was significantly accelerated in the $PRAK^{-/-}$ mice as compared to their $PRAK^{+/+}$ littermates, with a median tumor-free survival of 160 days (Figure 1A). Tumor development was also enhanced in the $PRAK^{+/-}$ animals, although only to a moderate level (with a median survival of 205 days). Western blot analysis of the spleens of these mice showed that these mice mostly expressed expected levels of PRAK and N-Ras (Figure 1B), indicating that PRAK suppresses oncogenic *ras*-induced hematopoietic tumorigenesis in mice. It is of interest to note that in some of the wild type tumors, PRAK expression was reduced to similar levels to that in the $PRAK^{+/-}$ tumors. This finding suggests that at least a subset of wild type mice developed tumors as a result of spontaneous reduction in PRAK expression. The other $PRAK^{+/+}$ tumors retained normal,

wild type PRAK expression, raising a possibility that mutations might have occurred in other components of the PRAK-mediated signaling pathway.

PRAK deletion accelerates formation of hematopoietic tumors of both myeloid and T-lymphoid origins

It has been reported that while the *Eμ-N-Ras*^{G12D} mice develop hematopoietic tumors of either myeloid or T-lymphoid origin, deletion of the *p53* or *Suv39h1* gene mainly enhances the development of T-cell lymphomas (15). We thus analyzed the origin of the tumors from PRAK-deficient *Eμ-N-Ras*^{G12D} animals, by immunogenotyping the cell types in hematopoietic compartments and analyzing the organs infiltrated by tumors. Consistent with previous reports, about 80% of the tumors developed in wild type mice were of myeloid origin, and 20% of these tumors were of T-lymphoid origin. Although heterozygous deletion of p53 increased the incidence of T-cell lymphoma to 45%, PRAK deficiency did not significantly alter the ratio between the 2 types of hematopoietic tumors (Table 1), despite the shortened disease latency in PRAK$^{+/-}$ and PRAK$^{-/-}$ animals (Figure 1A).

Detailed analysis revealed no difference in tumor characteristics between wild type and PRAK-deficient mice. The T-cell lymphomas from both wild type and PRAK-deficient animals were usually associated with enlarged spleen containing increased percentage of T-cells (CD3-positive), enlarged lymph nodes and thymus containing almost exclusively T-cells, and increased percentage of T-cells in bone marrow (Figure 2A, Table 2). The myeloid malignancies in PRAK$^{+/+}$, PRAK$^{+/-}$ and PRAK$^{-/-}$ mice all infiltrated spleen and liver (an organ not involved in T-cell lymphomas) (Figure 2A, 2B), and displayed increased percentage of CD11b^{+}GR-1^{-} myeloid cells in bone marrow and spleen (Table 3). In addition, peripheral blood analysis revealed signs of anemia in the myeloid tumor-bearing mice, while the white blood cell (including lymphocyte and myeloid cell) counts appeared to be normal (Figure 2C).

Therefore, PRAK deficiency accelerates the onset of N-Ras^{G12D}-induced hematopoietic cancer development without altering the spectrum or characteristics of the tumors. Our results thus suggest that PRAK functions as a tumor suppressor in hematopoietic cells of either myeloid or T-lymphoid lineage.

PRAK deficiency confers proliferative advantage in hematopoietic cells transduced with oncogenic *ras*

To investigate the cellular mechanism underlying the enhanced hematopoietic cancer development in PRAK deficient mice, we isolated hematopoietic cells from the spleen of PRAK$^{+/+}$, PRAK$^{+/-}$ and PRAK$^{-/-}$ littermates that did not carry the *N-ras*^{G12D} transgene, and transduced them with an oncogenic *ras* allele, *H-ras*^{G12V} or *N-ras*^{G12D} (Figure 3A, insert). While wild type cells also attained a higher proliferation rate upon transduction of either of the activated *ras* alleles as compared to a vector control, *ras*-induced cell proliferation was much more robust in PRAK deficient cells than in wild type cells (Figure 3A). We also examined the ability of these cells to grow and form colonies in semisolid media (Figure 3B, 3C). Cells failed to form any colonies on soft agarose in the absence of oncogenic *ras*, regardless of the PRAK status (Figure 3B). *H-ras*^{G12V} and *N-ras*^{G12D} promoted the formation of a number of small colonies in wild type cells; however, the colony formation by PRAK deficient cells transduced with activated *ras* was significantly increased in both size (Figure 3B) and quantity (Figure 3C), as compared to the wild type cells. These results demonstrate that loss of PRAK cooperates with oncogenic *ras* to induce proliferation and tumorigenesis in hematopoietic cells, suggesting that PRAK, when present in cells, suppresses *ras*-mediated cell proliferation and oncogenic transformation.

PRAK deficiency abrogates the induction of senescence markers by oncogenic *ras*

It was reported that activated *ras* induces senescence in primary splenocytes, which acts as a barrier ito lymphoma development (15). Our previous finding that PRAK suppresses skin carcinogenesis by mediating senescence (17) prompted us to investigate a possible role of PRAK-mediated senescence in hematopoietic cell transformation. However, we failed to detect a growth inhibition by oncogenic *ras* in either wild type or PRAK deficient splenocytes (Figure 3A). Instead, *ras* induced an increase in proliferation in these cell populations. In addition, neither wild type nor PRAK-deficient splenocytes displayed elevated percentage of cells positive for a senescence marker, senescence-associated β-galactosidase (SA-β-gal), upon transduction of activated *ras* alleles (data not shown). Nevertheless, oncogenic *ras* induced accumulation of other senescence markers, including DcR2, $p16^{INK4a}$ and $p19^{ARF}$ (12, 13, 22), and the induction of these senescence markers by *ras* was either abolished or greatly reduced in $PRAK^{-/-}$ splenocytes (Figure 4A). While the reason why activated *ras* fails to induced proliferative arrest and SA-β-gal is unclear, our data suggest that a PRAK-dependent senescence response may be at least partly responsible, although it may not be the major mechanism, for the tumor suppressing function of PRAK in hematopoietic cells.

PRAK deficiency enhances oncogenic *ras*-induced soft agar colony formation in splenocytes through hyper-activation of the JNK pathway

Previous studies revealed that p38α negatively regulates the proliferation of several cell types including fetal myeloid cells, and that targeted deletion of p38α enhances the proliferation of these cells and promotes cancer development by inducing hyper-activation of the JNK pathway (6). These reports raise a possibility that PRAK, as a downstream substrate of p38, may participate in the regulation of the JNK pathway and cell proliferation by p38. We thus examined the status of JNK activation in primary splenocytes transduced with oncogenic *ras* (Figure 4A). Indeed, $N\text{-}Ras^{G12D}$ alone induced a moderate increase in the protein levels of phospho-JNK, c-Jun, and a c-Jun downstream target cyclin D1. PRAK deletion alone also caused a weak, but consistent induction of these proteins. However, the combination of $N\text{-}Ras^{G12D}$ and PRAK deficiency synergistically led to a much higher level of induction of the JNK-c-Jun-cyclin D1 pathway (Figure 4A). In contrast, PRAK deletion had no effect on the activating phosphorylation of ERK and AKT induced by oncogenic *ras* (Figure 4A). Furthermore, treatment of the splenocytes with a JNK inhibitor SP600125, or transduction of these cells with shRNAs that effective silenced the expression of both JNK1 and JNK2 (Figure 4C, insert), strongly inhibited the induction of soft agar colony formation by oncogenic *ras* alone or by the combination of oncogenic *ras* and PRAK deficiency (Figure 4B, 4C). Thus, the induction of colony formation by oncogenic *ras* and the ability of PRAK deficiency to further promote oncogenic *ras*-induced colony formation both rely on activation of JNK. In addition, PRAK deficiency also enhanced proliferation of Eμ-$N\text{-}Ras^{G12D}$ splenocytes in vitro in a JNK-dependent fashion (Figure 4D). Together, these data suggest that PRAK-mediated inhibition of JNK activation contributes to suppression of tumorigenesis in hematopoietic compartments.

To gain insights into the mechanism for PRAK-mediated JNK inhibition, we examined the expression of a leukocyte-specific adaptor protein Grap2. Previous studies demonstrate that that Grap2 interacts with and enhances the activity of hematopoietic progenitor kinase 1 (HPK1), which in turn activates JNK and promotes proliferation in hematopoietic cells (6, 23). We found that Grap2 expression was induced by oncogenic *ras* to a much higher level in $PRAK^{-/-}$ splenocytes than in wild type cells (Figure 4E), suggesting that PRAK inhibits JNK by suppressing the Grap2-HPK1 circuit.

We previously showed that in a skin cancer model, PRAK suppressed carcinogenesis by inducing the tumor suppressing activity of p53 through phosphorylation of p53 at Ser37(17). Oncogenic *ras* induced total p53 protein levels in both wild-type and PRAK$^{-/-}$ splenocytes (Figure 4F, top panels); however, when the protein loading was adjusted to achieve comparable amounts of total p53 levels, we failed to detect any increase in the phospho-p53-Ser37 level in either wild-type or PRAK$^{-/-}$ splenocytes by Western blot analysis (Figure 4F, bottom panels). These indicate that the Ras-PRAK-p53Ser37 axis is not operative in splenocytes, suggesting that PRAK deletion accelerates *ras*-mediated hematopoietic cancer development through a p53Ser37-independent mechanism.

PRAK deficiency leads to hyper-activation of JNK in mice

To determine whether the hyper-activation of JNK mediated by PRAK deficiency occurs in vivo, the activated form of JNK (phospho-JNK-T183/Y185) was analyzed in both hematopoietic tumors and normal spleens by immunohistochemistry. We initially examined hematopoietic tumors isolated at the terminal illness from the spleens of PRAK$^{+/+}$, PRAK$^{+/-}$ and PRAK$^{-/-}$ littermates carrying the *N-ras*^{G12D} transgene. Compared to the PRAK$^{+/+}$ tumors, the amount of cells positive for phospho-JNK increased in PRAK$^{+/-}$ tumors, and further rose to a even higher level in PRAK$^{-/-}$ tumors (Figure 5A). To rule out the possibility that the increased phospho-JNK levels were associated with infiltrated tumor cells, a group of 6-month-old PRAK$^{+/+}$ and PRAK$^{-/-}$ littermates with or without the *N-ras*^{G12D} transgene were examined before any disease symptom was observed in the *N-ras*^{G12D} animals. Again, although the *N-ras*^{G12D} transgene induced an increase in the number of phospho-JNK positive cells in both PRAK$^{+/+}$ and PRAK$^{-/-}$ mice as compared to those without the transgene, the induction was much more prominent in the PRAK$^{-/-}$ than the PRAK$^{+/+}$ background (Figure 5B, top panel). Moreover, in the absence of the *N-ras*^{G12D} transgene, PRAK deficiency also significantly, although moderately, augmented the number of phospho-JNK positive cells in spleen (Figure 5B, top panel), even though these mice do not develop cancer without *N-ras*^{G12D}. This observation thus strongly suggests that the positive effect of PRAK deficiency on JNK activation is not restricted to tumor cells, but occurs also in normal hematopoietic cells and thus serves as the cause, rather than the consequence, of enhanced hematopoietic tumorigenesis. Supporting this notion, the enhancement in JNK activation by PRAK deficiency was observed in the spleens of mice harboring the *N-ras*^{G12D} transgene in as early as week-9 after birth, a time well before the onset of cancer in any mice, as determined by both immunohistochemical and Western blot analyses (Figure 5C). Furthermore, induction of phospho-JNK by the *N-ras*^{G12} transgene or PRAK deficiency, and the hyper-activation of JNK by both, strongly correlated with the increases in the number of cells positive for a proliferation marker Ki-67 (Figure 5B, top and bottom panels), suggesting that activation of JNK promotes the proliferation of normal hematopoietic cells as well as tumor cells, and contributes to enhanced hematopoietic cancer development.

Discussion

We previously demonstrated that PRAK suppresses DMBA-induced skin carcinogenesis in mice (17). In the current study, we show that PRAK also inhibits hematopoietic cancer development in mice harboring an activated *ras* allele, indicating that the tumor suppressing activity of PRAK operates in multiple tissues. This is consistent with the ubiquitous expression pattern of PRAK in tissues including skin and hematopietic cells (17, 24). Analysis of the tumors formed in the *Eμ-N-Ras*^{G12D} transgenic mice indicated that PRAK deficiency accelerated the formation of tumors of both lymphoid and myeloid origins, suggesting that PRAK serves as a guardian against tumorigenesis in both hematopoietic lineages. Supporting the role of PRAK in inhibiting hematopoietic cancer development,

hematopoietic cells isolated from PRAK-deficient spleens attained a faster proliferation rate and enhanced ability of form colonies on semi-solid medium upon transduction of oncogenic *ras* alleles, as compared to those from wild type animals.

Enhanced hematopoietic tumorigenesis correlates with hyper-activation of the JNK pathway by PRAK deficiency in both mouse spleen tissues and ex vivo cultivated splenocytes. In vivo, enhanced JNK activation by PRAK deficiency was detected in the spleens of *Eμ-N-Ras*^{G12D} transgenic animals from well before the disease onset all the way to the terminal illness, and in normal spleens from the non-transgenic littermates. These results suggest that PRAK suppresses JNK activity in hematopoietic tumor cells as well as normal hematopoietic cells. The pro-mitogenic and pro-oncogenic role of the JNK pathway has been well established in multiple cell types including lymphoma cells (6, 25-27). Indeed, we found that JNK activation correlates with enhanced proliferation of hematopoietic cells in vivo and in vitro, as revealed by a higher number of Ki-67-positive cells in spleens and an increased proliferation rate in splenocytes, respectively, and that PRAK deficiency promotes oncogenic *ras*-induced soft agar colony formation in a JNK-dependent manner. These findings suggest that hyper-activation of the JNK pathway plays a key role in the acceleration of hematopoietic cancer development by PRAK deletion. Supporting this notion, several papers have reported that p38 arrests cell proliferation and suppresses tumorigenesis by antagonizing the JNK pathway (6, 29). Interestingly, despite the general mitogenic activity of JNKs demonstrated by multiple studies, it was found that JNK1 negatively regulates T-cell receptor-initiated proliferation of CD4 helper (T_H) cells (28), suggesting that the function of this pathway may differ in response to distinct stimuli such as oncogenic signals and T-cell receptor activation.

In the previous study, we found that PRAK suppresses skin carcinogenesis by mediating oncogene induced senescence (17). PRAK-mediated senescence may also at least partially contribute to the suppression of hematopoietic tumorigenesis. Although we failed to observe growth arrest in hematopoietic cells transduced with oncogenic *ras*, at least a subset of senescence markers were induced in a PRAK-dependent manner. Although we do not understand the precise reason why activated *ras* fails to induce growth arrest despite the obvious PRAK-dependent induction of some senescence markers, it is possible that induction of senescence occurs only in a subpopulation of cells, while the remaining cells acquire a higher proliferation rate due to the moderate activation of JNK by oncogenic *ras* alone. As a result, the growth arrest in this subpopulation of senescent cells may have been obscured by the increased proliferation of the other cells in the growth curve assay, even though the more sensitive Western blot analysis detected alterations in senescence markers. It remains to be determined whether hyper-activation of JNK in PRAK deficient hematopoietic cells leads to disruption of *ras*-induced senescence, or *ras*-induced accumulation of senescence markers. However, the fact that activated *ras* alone causes moderate JNK activation and increased levels of senescence markers at the same time argues against a role of JNK activation in senescence bypass. Taken together with the well-established role of JNK in promoting cell proliferation, our data are consistent with the notion that JNK hyper-activation by PRAK deficiency contributes to accelerated tumorigenesis by enhancing cell proliferation, rather than by disrupting senescence, in hematopoietic compartments. On the other hand, PRAK-mediated senescence may only occur in a small subpopulation of hematopoietic cells, and thus is unlikely to be the major mechanism underlying the tumor suppressing function of PRAK in this system.

Several recent papers reported hematopoietic malignancies in mice expressing oncogenic *N-ras*^{G12D} from the endogenous locus (30-32). In these mice, a loxP-STOP-loxP (LSL)-N-ras^{G12D} allele was knocked into the *N-ras* locus, and its expression was induced specifically in hematopoietic cells by Mx1-Cre. The *Mx1-Cre, LSL-Nras*^{G12D} mice initially developed

an indolent myeloproliferative disorder (MPD) with elevated white blood cell counts, splenomegaly and myeloid ($CD11b^+GR1^+$) infiltration of bone marrow and spleen, and eventually die of a diverse spectrum of hematologic cancers including MPD and histiocytic sarcoma with liver and spleen enlargement. Similar to these studies, more than 80% of the *Eμ-N-ras*^{G12D} mice died of histiocytic sarcoma with myeloid infiltration in liver, spleen and bone marrow, while the remaining developed T-cell lymphoma. However, in contrast to the other model, the myeloid cells infiltrating bone marrow and spleen are $CD11b^+GR1^-$, instead of $CD11b^+GR1^+$, in the myeloid tumor-bearing *Eμ-N-ras*^{G12D} mice. In addition, the myeloid disease in *Eμ-N-ras*^{G12D} mice is not accompanied by increased white blood cell counts in peripheral blood. These differences are likely due to the different promoters used to drive *N-ras*^{G12D} expression in these studies. Although Mx1 and Eμ are both hematopoietic promoters, their specificity may differ in distinct subtypes of hematopoietic cells, leading to differential activation of *N-ras* in these cells. In addition, the endogenous *N-ras* promoter and the Eμ promoter may drive different expression levels of *N-ras*^{G12D}. Furthermore, as suggested by Wang et al for the *Mx1-Cre, LSL-Nras*^{G12D} mice (32), the genesis of histiocytic sarcoma with liver involvement may require simultaneous expression of oncogenic *N-ras* in both hematopoietic cells and the hepatic microenvironment. While this is also likely to be true for the *Eμ-N-ras*^{G12D} mice, our finding that PRAK deficiency promotes JNK-dependent proliferation and colony formation of primary splenocytes suggest that the cell autonomous effect of *N-ras*^{G12D} in hematopietic cells at least partly contributes to enhanced tumor formation in this model.

Acknowledgments

We thank Dr. A. W. Harris (Walter and Eliza Hall Institute of Medical Research, Australia) for providing the Eμ-N-Ras^{G12D} strain and Dr. Carol Prives (Columbia University) for an antibody against mouse p53 phosphorylated at S37. This work was supported by grants from NIH (CA106768, CA131231 and RR025744 to P.S., and an international collaborative grant from NSF China (30828019, P.S. and J.H.). This Scripps manuscript number is 21440.

References

(1). Han J, Lee JD, Bibbs L, Ulevitch RJ. A MAP kinase targeted by endotoxin and hyperosmolarity in mammalian cells. Science. 1994; 265:808–11. [PubMed: 7914033]

(2). Rouse J, Cohen P, Trigon S, Morange M, onso-Llamazares A, Zamanillo D, et al. A novel kinase cascade triggered by stress and heat shock that stimulates MAPKAP kinase-2 and phosphorylation of the small heat shock proteins. Cell. 1994; 78:1027–37. [PubMed: 7923353]

(3). Lee JC, Laydon JT, McDonnell PC, Gallagher TF, Kumar S, Green D, et al. A protein kinase involved in the regulation of inflammatory cytokine biosynthesis. Nature. 1994; 372:739–46. [PubMed: 7997261]

(4). Ono K, Han J. The p38 signal transduction pathway: activation and function. Cell Signal. 2000; 12:1–13. [PubMed: 10676842]

(5). Han J, Sun P. The pathways to tumor suppression via route p38. Trends Biochem Sci. 2007; 32:364–71. [PubMed: 17624785]

(6). Hui L, Bakiri L, Mairhorfer A, Schweifer N, Haslinger C, Kenner L, et al. p38alpha suppresses normal and cancer cell proliferation by antagonizing the JNK-c-Jun pathway. Nat Genet. 2007; 39:741–9. [PubMed: 17468757]

(7). Ventura JJ, Tenbaum S, Perdiguero E, Huth M, Guerra C, Barbacid M, et al. p38alpha MAP kinase is essential in lung stem and progenitor cell proliferation and differentiation. Nat Genet. 2007; 39:750–8. [PubMed: 17468755]

(8). Bulavin DV, Demidov ON, Saito S, Kauraniemi P, Phillips C, Amundson SA, et al. Amplification of PPM1D in human tumors abrogates p53 tumor-suppressor activity. Nat Genet. 2002; 31:210–5. [PubMed: 12021785]

(9). Bulavin DV, Phillips C, Nannenga B, Timofeev O, Donehower LA, Anderson CW, et al. Inactivation of the Wip1 phosphatase inhibits mammary tumorigenesis through p38 MAPK-mediated activation of the p16(Ink4a)-p19(Arf) pathway. Nat Genet. 2004; 36:343–50. [PubMed: 14991053]

(10). Shi Y, Gaestel M. In the cellular garden of forking paths: how p38 MAPKs signal for downstream assistance. Biol Chem. 2002; 383:1519–36. [PubMed: 12452429]

(11). Shay JW, Wright WE. Senescence and immortalization: role of telomeres and telomerase. Carcinogenesis. 2005; 26:867–74. [PubMed: 15471900]

(12). Serrano M, Lin AW, McCurrach ME, Beach D, Lowe SW. Oncogenic ras provokes premature cell senescence associated with accumulation of p53 and p16INK4a. Cell. 1997; 88:593–602. [PubMed: 9054499]

(13). Collado M, Gil J, Efeyan A, Guerra C, Schuhmacher AJ, Barradas M, et al. Tumour biology: senescence in premalignant tumours. Nature. 2005; 436:642. [PubMed: 16079833]

(14). Michaloglou C, Vredeveld LC, Soengas MS, Denoyelle C, Kuilman T, van der Horst CM, et al. BRAFE600-associated senescence-like cell cycle arrest of human naevi. Nature. 2005; 436:720–4. [PubMed: 16079850]

(15). Braig M, Lee S, Loddenkemper C, Rudolph C, Peters AH, Schlegelberger B, et al. Oncogene-induced senescence as an initial barrier in lymphoma development. Nature. 2005; 436:660–5. [PubMed: 16079837]

(16). Chen Z, Trotman LC, Shaffer D, Lin HK, Dotan ZA, Niki M, et al. Crucial role of p53-dependent cellular senescence in suppression of Pten-deficient tumorigenesis. Nature. 2005; 436:725–30. [PubMed: 16079851]

(17). Sun P, Yoshizuka N, New L, Moser BA, Li Y, Liao R, et al. PRAK Is Essential for ras-Induced Senescence and Tumor Suppression. Cell. 2007; 128:295–308. [PubMed: 17254968]

(18). Harris AW, Langdon WY, Alexander WS, Hariharan IK, Rosenbaum H, Vaux D, et al. Transgenic mouse models for hematopoietic tumorigenesis. Curr Top Microbiol Immunol. 1988; 141:82–93. [PubMed: 3215058]

(19). Khatlani TS, Wislez M, Sun M, Srinivas H, Iwanaga K, Ma L, et al. c-Jun N-terminal kinase is activated in non-small-cell lung cancer and promotes neoplastic transformation in human bronchial epithelial cells. Oncogene. 2007; 26:2658–66. [PubMed: 17057737]

(20). Sun P, Dong P, Dai K, Hannon GJ, Beach D. p53-independent role of MDM2 in TGF-beta1 resistance. Science. 1998; 282:2270–2. [PubMed: 9856953]

(21). Hannon GJ, Sun P, Carnero A, Xie LY, Maestro R, Conklin DS, et al. MaRX: an approach to genetics in mammalian cells. Science. 1999; 283:1129–30. [PubMed: 10075573]

(22). Collado M, Serrano M. The power and the promise of oncogene-induced senescence markers. Nat Rev Cancer. 2006; 6:472–6. [PubMed: 16723993]

(23). Ma W, Xia C, Ling P, Qiu M, Luo Y, Tan TH, et al. Leukocyte-specific adaptor protein Grap2 interacts with hematopoietic progenitor kinase 1 (HPK1) to activate JNK signaling pathway in T lymphocytes. Oncogene. 2001; 20:1703–14. [PubMed: 11313918]

(24). New L, Jiang Y, Zhao M, Liu K, Zhu W, Flood LJ, et al. PRAK, a novel protein kinase regulated by the p38 MAP kinase. EMBO J. 1998; 17:3372–84. [PubMed: 9628874]

(25). Schreiber M, Kolbus A, Piu F, Szabowski A, Mohle-Steinlein U, Tian J, et al. Control of cell cycle progression by c-Jun is p53 dependent. Genes Dev. 1999; 13:607–19. [PubMed: 10072388]

(26). Sabapathy K, Hochedlinger K, Nam SY, Bauer A, Karin M, Wagner EF. Distinct roles for JNK1 and JNK2 in regulating JNK activity and c-Jun-dependent cell proliferation. Mol Cell. 2004; 15:713–25. [PubMed: 15350216]

(27). Lizundia R, Chaussepied M, Huerre M, Werling D, Di Santo JP, Langsley G. c-Jun NH2-terminal kinase/c-Jun signaling promotes survival and metastasis of B lymphocytes transformed by Theileria. Cancer Res. 2006; 66:6105–10. [PubMed: 16778183]

(28). Dong C, Yang DD, Wysk M, Whitmarsh AJ, Davis RJ, Flavell RA. Defective T cell differentiation in the absence of Jnk1. Science. 1998; 282:2092–5. [PubMed: 9851932]

(29). Chen G, Hitomi M, Han J, Stacey DW. The p38 pathway provides negative feedback for Ras proliferative signaling. J Biol Chem. 2000; 275:38973–80. [PubMed: 10978313]

(30). Li Q, Haigis KM, McDaniel A, Harding-Theobald E, Kogan SC, Akagi K, et al. Hematopoiesis and leukemogenesis in mice expressing oncogenic NrasG12D from the endogenous locus. Blood. 2011; 117:2022–32. [PubMed: 21163920]

(31). Wang J, Liu Y, Li Z, Wang Z, Tan LX, Ryu MJ, et al. Endogenous oncogenic Nras mutation initiates hematopoietic malignancies in a dose- and cell type-dependent manner. Blood. 2011; 118:368–79. [PubMed: 21586752]

(32). Wang J, Liu Y, Li Z, Du J, Ryu MJ, Taylor PR, et al. Endogenous oncogenic Nras mutation promotes aberrant GM-CSF signaling in granulocytic/monocytic precursors in a murine model of chronic myelomonocytic leukemia. Blood. 2010; 116:5991–6002. [PubMed: 20921338]

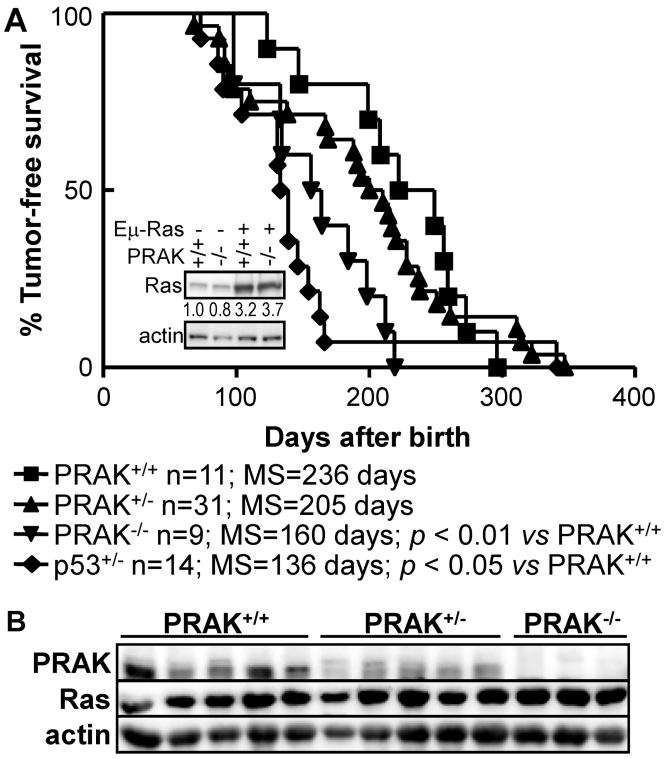

Figure 1.

PRAK deficiency accelerates hematopoietic cancer development in *Eμ-N-Ras*^{G12D} transgenic mice.

(A) Kaplan-Meier plots for tumor-free survival of *Eμ-N-Ras*^{G12D}*;PRAK*$^{+/+}$, *Eμ-N-Ras*^{G12D}*;PRAK*$^{+/-}$ and *Eμ-N-Ras*^{G12D}*;PRAK*$^{-/-}$ littermates. Number of mice for each genotype (*n*), median survival (MS) and statistical significance in log-rank test (*p*) are shown. *Insert*, Western blot analysis of N-Ras expression levels in splenocytes of mice of indicated genotypes. Relative Ras expression levels are indicated.

(B) Western blot analysis of spleens of tumor-bearing *Eμ-N-Ras*^{G12D}*;PRAK*$^{+/+}$, *Eμ-N-Ras*^{G12D}*;PRAK*$^{+/-}$ and *Eμ-N-Ras*^{G12D}*;PRAK*$^{-/-}$ littermates.

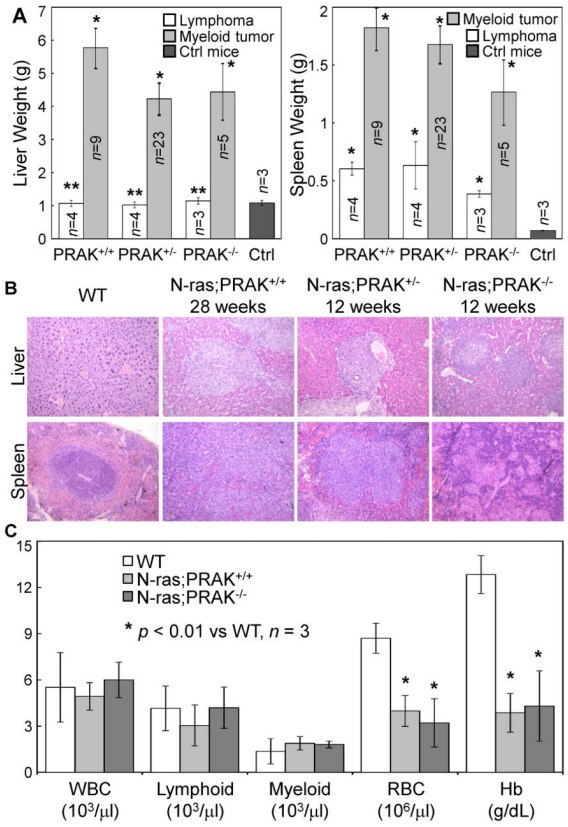

Figure 2.

Characterization of T-lymphoid and myeloid malignancies in *Eμ-N-Ras*^{G12D} transgenic mice. (A) Average weight of liver (left) and spleen (right) from wild type control mice (Ctrl) or *Eμ-N-Ras*^{G12D} transgenic mice of indicated PRAK genotypes with lymphomas or myeloid tumors at terminal illness. Numbers are mean ± SEM for indicated number of organs (n). Statistical significance was determined by Student t test. * $p < 0.05$; ** $p > 0.8$, for mice with tumors vs. wild type mice (Ctrl).

(B) Hematoxylin/Eosin (H/E) staining of liver and spleen sections from normal wild type mice or myeloid tumor-bearing *Eμ-N-Ras*^{G12D} transgenic mice with indicated genotypes.

(C) Peripheral blood analysis in normal wild type mice and myeloid tumor-bearing *Eμ-N-Ras*^{G12D} transgenic mice with indicated PRAK genotypes, showing mean ± SD of white blood cell count (WBC), lymphocyte and myeloid cell counts, red blood cell counts (RBC) and hemoglobin concentrations (Hb) for 3 mice. . * $p < 0.01$ for *Eμ-N-Ras*^{G12D} transgenic mice vs. wild type mice determined by Student t test.

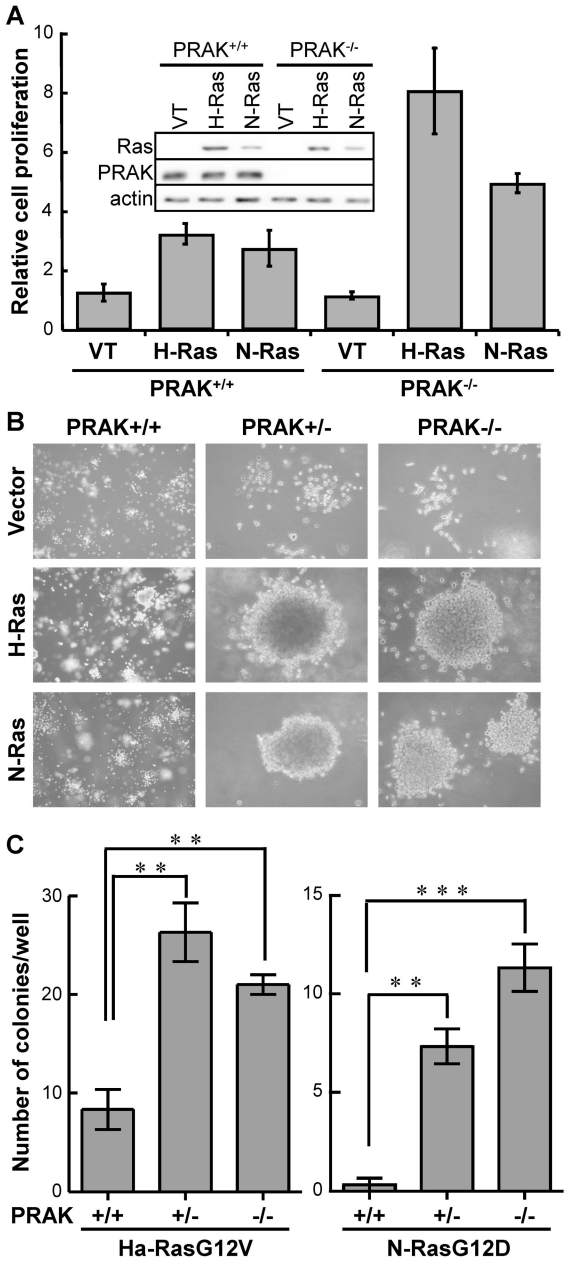

Figure 3.

PRAK deficiency enhances oncogenic *ras*-induced proliferation and colony formation in primary splenocytes.

(A) PRAK deficiency enhances oncogenic *ras*-induced proliferation. Splenocytes isolated from $PRAK^{+/+}$ or $PRAK^{-/-}$ mice were transduced with vector control (VT), $H\text{-}Ras^{G12V}$ (H-Ras) o*r* $N\text{-}Ras^{G12D}$ (N-Ras), and plated in triplicates onto 12-well plates at a density of 4×10^4 cells/well in NIH3T3-conditioned splenocyte medium. Cell numbers were counted 6 days later, and normalized to the number of vector-transduced cells. *Insert*, Western blot analysis showing *ras*, PRAK and actin expression levels in these cell lines.

(B, C) PRAK deficiency enhances oncogenic *ras*-induced colony formation on semi-solid medium. Splenocytes isolated from $PRAK^{+/+}$ or $PRAK^{-/-}$ mice were transduced with vector control (VT), $H\text{-}Ras^{G12V}$ (H-Ras) *or* $N\text{-}Ras^{G12D}$ (N-Ras), and plated in triplicates onto 6-

well plates at a density of 1×10^4 cells/well in NIH3T3-conditioned splenocyte medium containing 0.3% low-melting-point agarose. Cells were stained with 0.02% Giemsa in PBS and photographed 3 weeks after seeding (B). Numbers of colonies were quantified using the AlphaView image quantification software (Cell Biosciences) (C).

(A, C) Numbers are mean ± SD for triplicates. Statistical significance was determined by Student t test. ** $p < 0.001$; *** $p < 0.0001$.

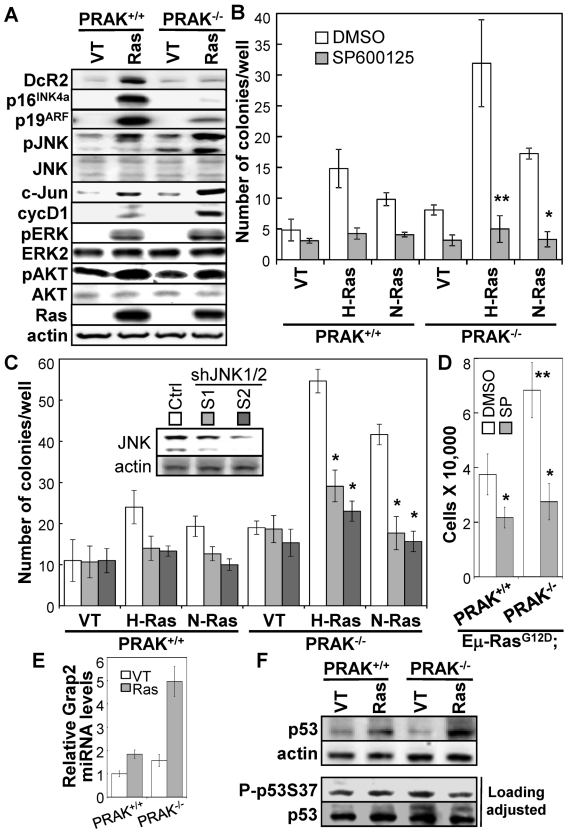

Figure 4.

PRAK deficiency enhances oncogenic *ras*-induced cell proliferation and colony formation on semi-solid medium by hyper-activating the JNK pathway.

(A) Western blot analysis of $PRAK^{+/+}$ and $PRAK^{-/-}$ splenocytes 4 days after transduction with vector control (VT) or $N\text{-}Ras^{G12D}$ (Ras).

(B) $PRAK^{+/+}$ and $PRAK^{-/-}$ splenocytes were transduced with vector control (VT), $H\text{-}Ras^{G12V}$ (H-Ras) *or* $N\text{-}Ras^{G12D}$ (N-Ras), and plated in triplicates onto 6-well plates at a density of 1×10^4 cells/well in NIH3T3-conditioned splenocyte medium containing 0.3% low-melting-point agarose and 2 μM of SP600125 or DMSO.

(C) $PRAK^{+/+}$ and $PRAK^{-/-}$ splenocytes were cotransduced with pRetroSuper-shJNK1/2 (S1 or S2) or vector control (Ctrl) and $H\text{-}Ras^{G12V}$ (H-Ras), $N\text{-}Ras^{G12D}$ (N-Ras) or vector control (VT), and plated in triplicates onto 6-well plates at a density of 1×10^4 cells/well in NIH3T3-conditioned splenocyte medium containing 0.3% low-melting-point agarose. *Insert*, Western blot analysis showing knockdown of JNK1 and JNK2 by shRNA (S1 and S2) as compared to the control shRNA (Ctrl).

(B, C) Cells were stained with 0.02% Giemsa in PBS 3 week later, and numbers of colonies were quantified using the AlphaView software (Cell Biosciences). Numbers are mean ± SD for triplicates. Statistical significance was determined by Student t test. * $p < 0.005$ and ** $p < 0.01$, for Ras-SP600125 vs Ras-DMSO or Ras-shJNK vs Ras-Ctrl.

(D) Cell numbers were counted 4 days after 2×10^4 of Eμ-N-Ras^{G12D};$PRAK^{+/+}$ or Eμ-N-Ras^{G12D};$PRAK^{-/-}$ splenocytes were seeded onto 12-well plates and treated with control (DMSO) or 2 μM of SP600125 (SP). Numbers are mean ± SD for triplicates. Statistical significance was determined by Student t test. * $p < 0.05$ for SP600125 vs. DMSO; and ** $p < 0.02$ for Eμ-N-Ras^{G12D};$PRAK^{-/-}$ (DMSO) vs. Eμ-N-Ras^{G12D};$PRAK^{+/+}$ (DMSO).

(E) Relative levels of Grap2 mRNA in $PRAK^{+/+}$ or $PRAK^{-/-}$ splenocytes 4 days post transduction with vector control (VT) or $N\text{-}Ras^{G12D}$ (Ras) after normalization to GAPDH signals, as determined by quantitative real time PCR. Numbers are mean ± SD for triplicates.

(F) Western blot analysis of $PRAK^{+/+}$ and $PRAK^{-/-}$ splenocytes 4 days after transduction with vector control (VT) or $N\text{-}Ras^{G12D}$ (Ras). In the bottom 2 panels, sample volumes were adjusted to achieve comparable loading of total p53 protein levels.

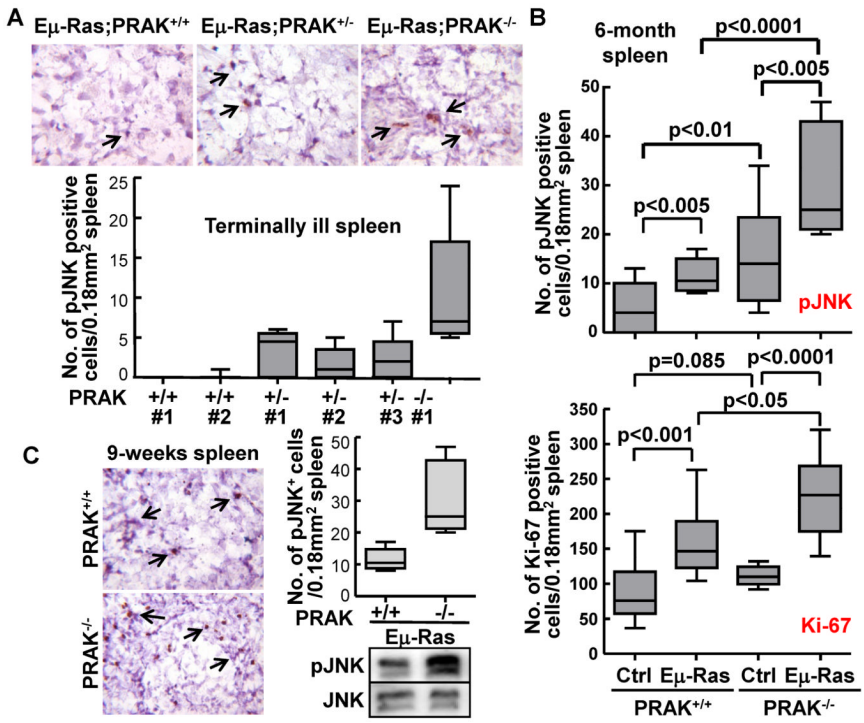

Figure 5.

PRAK deficiency leads to hyper-activation of JNK and increased cell proliferation in vivo. Immunohistochemical analysis of phospho-JNK-T183/Y185 (A, B-top panel, and C) and Ki-67 (B-bottom panel) in spleens of terminally ill *Eμ-N-Ras^{G12D};PRAK$^{+/+}$*, *Eμ-N-Ras^{G12D};PRAK$^{+/-}$*, and *Eμ-N-Ras^{G12D};PRAK$^{-/-}$* littermates (A), 6-month-old *PRAK$^{+/+}$*, *Eμ-N-Ras^{G12D};PRAK$^{+/+}$*, *PRAK$^{-/-}$*, and *Eμ-N-Ras^{G12D};PRAK$^{-/-}$* littermates (B), or 9-week-old *Eμ-N-Ras^{G12D};PRAK$^{+/+}$* and *Eμ-N-Ras^{G12D};PRAK$^{-/-}$* littermates (C). *Arrows* indicate examples of cells positive for phospho-JNK (A-top panels and C-left panels), *Bar graphs* represent positive cells quantified under microscope in 20 randomly chosen 40X-fields. Numbers are mean ± SD. Statistical significance was determined by unpaired t test. Western blot analysis was performed to measure the phospho-JNK and JNK levels in spleens of 9-week-old *Eμ-N-Ras^{G12D};PRAK$^{+/+}$* and *Eμ-N-Ras^{G12D};PRAK$^{-/-}$* littermates (C-bottom right panels).

Table 1

Percentage of tumors of myeloid and lymphoid origins from mice of indicated genotypes harboring the *Eμ-N-Ras*^{G12D} transgene, determined by immunogenotyping of the tumor cells and the type of infiltrated organs.

	Tumor origin	%
PRAK$^{+/+}$ **(n=15)**	Myeloid*	80.0 %
	Lymphoid	20.0 %
PRAK$^{+/-}$ **(n=33)**	Myeloid	90.9 %
	Lymphoid	9.1 %
PRAK$^{-/-}$ **(n=9)**	Myeloid	77.8 %
	Lymphoid	22.2 %
p53$^{+/-}$ **(n=22)**	Myeloid	54.5 %
	Lymphoid	45.5 %

Table 2

Immunogenotyping of cells were isolated from indicated organs of wild type (WT) mice or lymphoid tumor-bearing *Eμ-N-Ras^{G12D};PRAK$^{+/+}$* and *Eμ-N-Ras^{G12D};PRAK$^{-/-}$* mice.

Marker	CD3+		B220+		CD11b+ GR-1−		CD11b+ GR-1+	
Tissue	**BM**	**SP**	**BM**	**SP**	**BM**	**SP**	**BM**	**SP**
N-ras;PRAK$^{+/+}$	61±8.7*	82±4.7*	2.7±1.0	7.4±1.7	4.1±0.6	3.5±0.9	27±6.7	1.9±0.5
N-ras;PRAK$^{-/-}$	56±6.4*	88±3.1*	3.3±0.5	3.6±1.0	2.0±0.8	1.4±0.5	34±7.0	2.3±0.6
WT	2.7±1.0	30±4.3	27±2.9	56±2.8	15±0.6	6.1±0.5	52±3.6	1.4±0.3

Numbers are means of percentage of cells positive for indicated hematopoietic cell markers ± SEM for 3 independent analyses for each organ type from each genotype. BM, bone marrow; SP, spleen.

$^{*}p < 0.05$ for *Eμ-N-Ras^{G12D}* transgenic mice vs. wild type mice determined by Student t test.

Table 3

Immunogenotyping of cells were isolated from indicated organs of wild type (WT) mice or myeloid tumor-bearing *Eμ-N-Ras^{G12D};PRAK$^{+/+}$* and *Eμ-N-Ras^{G12D};PRAK$^{-/-}$* mice.

Marker	CD3+		B220+		CD11b+ GR-1−		CD11b+ GR-1+	
Tissue	**BM**	**SP**	**BM**	**SP**	**BM**	**SP**	**BM**	**SP**
N-ras;PRAK$^{+/+}$	3.9±1.2	24±6.1	4.6±1.0	3.6±0.8	30±2.3*	66±6.7*	53±2.1	1.9±0.7
N-ras;PRAK$^{-/-}$	3.2±0.8	27±3.1	3.4±1.5	5.1±1.8	28±2.0*	63±7.6*	56±3.4	1.7±0.7
WT	2.7±1.0	30±4.3	27±2.9	56±2.8	15±0.6	6.1±0.5	52±3.6	1.4±0.3

Numbers are means of percentage of cells positive for indicated hematopoietic cell markers ± SEM for 3 independent analyses for each organ type from each genotype. BM, bone marrow; SP, spleen.

$^{*}p < 0.05$ for *Eμ-N-Ras^{G12D}* transgenic mice vs. wild type mice determined by Student t test.